Available online at www.sciencedirect.com

ScienceDirect

Proceedings of the Combustion Institute 36 (2017) 2919–2925

Proceedings of the Combustion Institute

www.elsevier.com/locate/proci

# Characterization of flame stabilization modes in an ethylene-fueled supersonic combustor using time-resolved CH* chemiluminescence

Yueming Yuan [a], Taichang Zhang [a], Wei Yao [a], Xuejun Fan [a,*], Peng Zhang [b]

[a] State Key Laboratory of High Temperature Gas Dynamics, Chinese Academy of Sciences, Beijing 100190, PR China
[b] Department of Mechanical Engineering, The Hong Kong Polytechnic University, Kowloon, Hong Kong

Received 4 December 2015; accepted 10 July 2016
Available online 19 July 2016

**Abstract**

Flame stabilization in a Ma = 2.5 direct-connect supersonic combustor was experimentally characterized with a fixed stagnation pressure of 1.0 MPa and wide ranges of stagnation temperature ($T_0$) from 1200 K to 1800 K and global equivalence ratio ($\Phi$) of ethylene/air from 0.1 to 0.8. Four typical flame stabilization modes were identified by using the time resolved CH* chemiluminescence and presented as a regime nomogram in the $T_0$–$\Phi$ parameter space. As increasing $T_0$, the range of $\Phi$ for the flame stabilization modes is widened and that for the oscillation mode is therefore narrowed. The widely used quasi-1D analysis, with the experimentally determined wall static pressure distribution as input parameters, suggests that the combustor operates in a scramjet mode when the flame is stabilized in the cavity shear layer and in a ramjet mode when the flame is in the jet-wake. The flame oscillation mode, observed only for a narrow range of $\Phi$, was found to correlate with the combustor transition between the scramjet and ramjet modes.


*Keywords:* Supersonic combustion; Flame stabilization; Stagtnation temperature; Gloabal equivalence ratio; CH* chemiluminesence

## 1. Introduction

Flame stablization in a wide range of flight Mach numbers, particularly from ramjet to scramjet, is critical to the application of dual-mode scramjet engines. The Damköhler number, defined as the ratio of the characteristic flow time to the reaction time, has been conventionally used to characterize non-premixed flame stabilization in high-speed flows [1]. For the flight Mach number $M_f = 6$–7, relatively high static temperatures appear in the combustor due to the well-known compression heating effect [2,3] and result in relatively large Damköhler numbers. As a result, combustion can be stabilized in the jet-wake of fuel injection and is controlled by the fuel/air mixing since the

* Corresponding author.
*E-mail address:* xfan@imech.ac.cn (X. Fan).

http://dx.doi.org/10.1016/j.proci.2016.07.040
1540-7489 

mixture tends to be auto-ignited at high static temperatures. For $M_f = 3$–4, the characteristic reaction time increases exponentially with the decrease of the static temperature, although the fuel/air mixing is enhanced due to the longer flow residence time. Consequently, the auto-ignition in the jet-wake of fuel injection becomes unlikely under such a condition; flameholders, such as cavities [4], steps [5], and struts [6], must be configured to create local low-speed regions, which can further prolong the flow residence time and in addtion provide hot radical pools to sustain combustion. For intermediate $M_f$, both the fuel/air mixing and the chemical reaction influence the flame stabilization.

Micka and Driscoll [7] experimentally studied a dual-mode ramjet/scramjet combustor fueled with either hydrogen or hydrogen/ethylene mixtures, and observed the stable flame either anchored in the cavity shear layer at relatively low stagnation temperatures or stabilized in the fuel jet-wake at higher stagnation temperatures. In the intermediate stagnation temperatures, the flame oscillates between the jet-wake and the cavity shear layer. For blended ethylene-hydrogen fuels, the transition from the cavity shear layer mode to the jet-wake mode occurs at higher stagnation temperatures. By using interferometric imaging, Fotia and Driscoll [9] experimentally observed the evolution of flame-holding behavior during the combustion mode transition and investigated the parameteric dependence of the transition on the stagnation temperature and the global equivalence ratio. Futhermore, the flame oscillations were observed under the operating conditions close to the scramjet-ramjet transition, which induce multiple cycles of the combustion mode transition [10]. Wang et al. [8] experimentally investigated the cavity-assisted hydrogen jet combustion and found out that the jet-wake mode is less stable compared with the combined cavity shear-layer/recirculation mode. Dalle et al. [11] obtained two mathematically possible sulutions near the ramjet-scramjet boundary, which however have not been verified by experimental studies. In spite of these worthy advances in understanding flame stabilization modes, the correlation between the initiation of transition instability and operating parameters has been not sufficiently studied.

Recently, Yuan et al. [12] studied the ethylene flame stabilization in a Ma = 2.5 model combustor with a fixed stagnation temperature of 1275 ± 25 K and a relatively small variation of fuel/air ratio from 0.26 to 0.41. Four typical streamwise locations of stablized flame were observed by using CH* chemiluminescence combined with pulsed schlieren flow visualization. Specifically, the flame was stabilized either in the cavity or in the shear layer when the local flow remains supersonic. When a short-lived thermal choking is formed around the fuel injector as a result of increasing the amount of fuel injection, the flame starts oscillating between the shear layer and the jet-wake. To further substantiate and extend their expererimental observations to a wider range of engines conditions, the present study aims to systematically characterize the flame stabilization modes by invesigating the influence of the stagnation temperature and the fuel/air global equivalence ratio. The interdependence between the observed flame stabilization modes and the combustion modes will be characterized in the study by using the time-resolved CH* chemilluminence and the widely-used quasi-1D flow analysis.

## 2. Experimental specifications and analysis

All the experiments were conducted in a Ma = 2.5 direct-connect test facility, which has been detailedly described in Zhang et al. [12–14]. The facility consists of a vitiated air supply system and a multipurpose supersonic model combustor. Supplied by burning hydrogen in air with oxygen replenishment, the vitiated air can have a stagnaiton temperature of 700–2200 K and a stagnation pressure of 0.6–4.5 MPa. As shown in Fig. 1, the model combustor of 1600 mm in length consists of four sections: a constant area isolator of 350 mm in length, 51 mm in height and 70 mm in width, and three divergent sections of 500, 400, and 350 mm in length and 1.3, 2.9, and 4.0° in expansion angle, respectively. An interchangeable, integrated fuel-injection/flameholder cavity module is installed on one side of the combustor. The cavity, having 12 mm in depth, 45° aft ramp and an overall length-to-depth ratio of 4, is located 611 mm downstream from the isolator entrance. An orifice of 4 mm in diameter for transverse ethylene injection is located 56 mm upstream from the cavity leading edge. Two orifices of 2.5 mm in diameter for transverse pilot hydrogen injection are located 8 mm upstream from the cavity leading edge. A pair of quartz windows facing the cavity module are installed on both sides of the combustor for optical access.

The stagnation pressure, $P_0$, and the stagntation temperature, $T_0$, of the vitiated airflow are measured by using the CYB-10S pressure transducer with the accuracy of 0.1% and the Type-B thermocouple with an exposed tip, respectively. The wall static pressures were measured through a number of pressure taps along the test section, each of which was instrumented with a Motorola MPX2200 pressure transducer with the uncertainty of 0.1%. The mass flow rates were controlled and measured by sonic nozzles, whose mass flow rate coefficients were calibrated to have an uncertainty of 1% for airflow and 5% for fuel flow. The relative error for the global equivalence ratio [9], Φ, defined as the one of furl/air flow rate ratio to that under the stoichiometric condition, was determined to be about ± 3%.

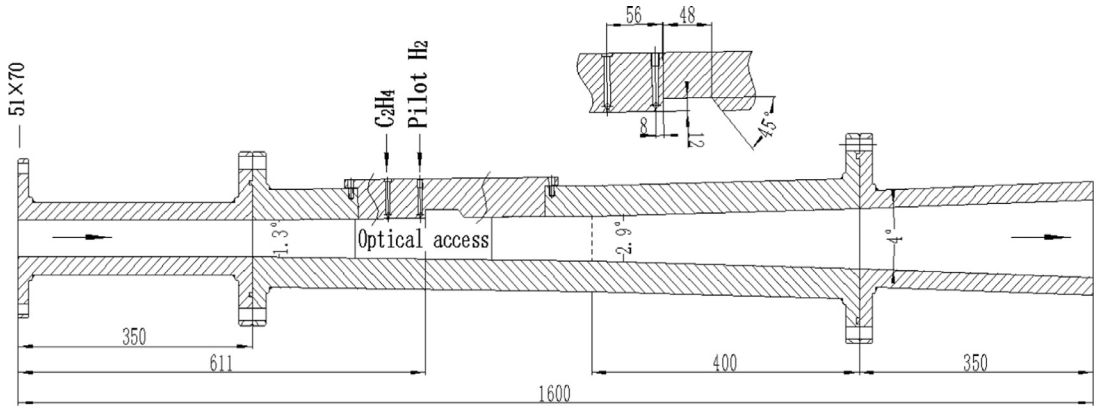


Fig. 1. Schematic of a dual-mode modal combustor (dimensions in mm).

As a nanosecond-lifetime intermediate species, $CH^*$ radical exists only in the fuel consumption layer [15–17] and $CH^*$ chemiluminescence of hydrocarbon flames can be therefore used to denote the primary reaction zone [18,19]. In the present study, $CH^*$ chemiluminescence was detected by using a high-speed camera v711 with 100 μs exposure time and 5000 fps, combined with a CH band-filter MF434-17. Each flame stabilization mode was analyzed statistically based on the mean and standard deviation of 5000 images, which can characterize the reaction zone and its variation, respectively. To facilitate the comparison between different combustion stabilization modes, the mean and standard deviation images were presented in pseudo-color with the same color-bar.

By virtue of the experimentally determiend wall static pressures and the widely used quasi-1D analysis of Heiser and Pratt [3], the streamwise variation of the flow Mach number, $M_a$, can be determined by

$$\frac{dM_a}{M_a dx} = \left[\frac{1+\frac{(\gamma-1)M_a^2}{2}}{1-M_a^2}\right] \times \left(-\frac{dA}{Adx} + \frac{1+\gamma M_a^2}{2}\frac{dT_t}{T_t dx}\right) \quad (1)$$

where that the flow is assumed to be frictionaless and uniform at any streamwise location with unknown cross section area $A$ (due to the unknown thickness of boundary layer) and total temperature $T_t$ including heat release. By using Heiser and Pratt's empirical formula for heat release and the measured static pressure distribution along the wall [20,21], Eq. (1) has been used [12,14] to estimate the Mach number distribution in the combustor; the uncertainty of the calculated Mach number is about ± 3%. Although the calcualted Mach number variation cannot completely describe the actual complex flows around the cavity and fuel injection, which are three dimensional in nature and affected by the complex interaction among the shock waves, combustion and boundary layer in the near-wall region, the quasi-1D analysis has been widely used in decades and proved to be an effective tool to help to analyze supersonic combustion experiments [9,10].

Table 1
Stagnation temperature ($T_0$) and global equivalence ratio (Φ) for various flame stabilization modes.

| Case | Flame stabilization modes | $T_0$/K | Φ |
|---|---|---|---|
| A | Inside the cavity | 1430 | 0.28 |
| B | Cavity shear layer | – | 0.41 |
| C | Jet-wake | – | 0.55 |
| D | Oscillation | – | 0.47 |
| E | Jet-wake | 1280 | – |
| F | Cavity shear layer | 1780 | – |

## 3. Results and discussions

### 3.1. Flame stabilization modes

To facilitate the following discussion, the experimental conditions for six representative cases of flame stabilization modes are summarized in Table 1. Specifically, Cases A-D have a fixed stagnation temperature of $T_0 = 1430 \pm 40$ K, while their global equivalence ratios, Φ, vary significantly from 0.28 to 0.55. Cases D–F have a fixed $\Phi = 0.47$ while their $T_0$ vary significantly between 1270 K and 1780 K. In all the cases, the stagnation pressure is fixed at $P_0 = 1.03 \pm 0.02$ MPa.

Figure 2 shows the flame mean and standard deviation images for Cases A–F. The corresponding wall static pressure profiles and calculated Mach number distributions are shown in Figs. 3 and 4, respectively. The coordinates are scaled by the isolator height (H = 51 mm) and the origin is located at the fuel injector (x/H = 0).

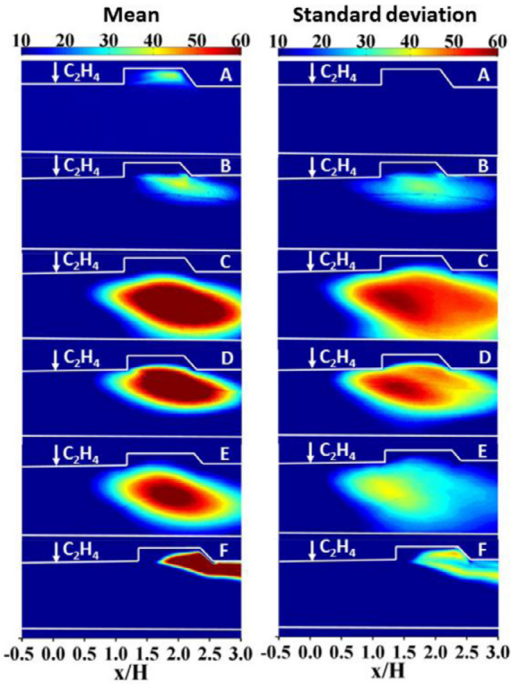


Fig. 2. Mean and standard deviation images for CH* chemiluminescence for Cases A–F.

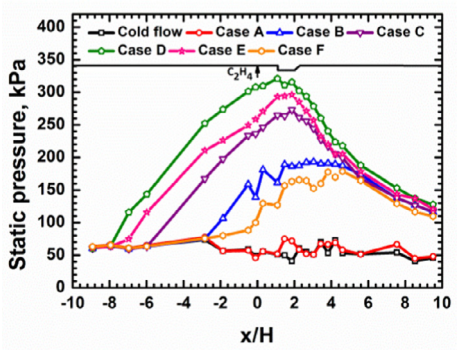


Fig. 3. Measured wall static pressure profiles for Cases A–F.

Case A with $\Phi = 0.28$ is often referred to as weak combustion [22,23] beause it caused only a slight rise of the static pressure, rendering the flow remains supersonic throughout the combustor. Therefore, the flame can be held only in the cavity with negligible spatial variation, as suggested by the small standard deviation of flame locations.

In Case B with $\Phi = 0.41$, the flame was observed in the cavity shear layer. The manifest flame variation around the cavity implies that a remarkable amount of heat release was produced to increase the temperature in cavity shear layer so that an intensive combustion can occur in the adjacent main

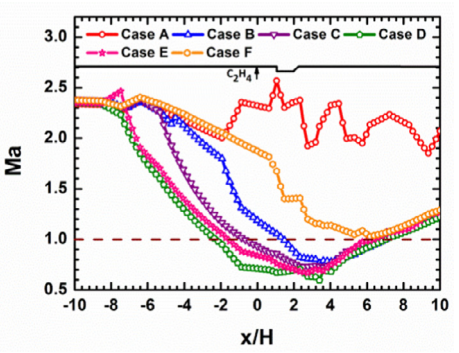


Fig. 4. Calculated Mach number distributions for Cases A–F.

flow. The pressure fluctuation between injector and cavity, as shown in Fig. 3, might attribute to the reflections of oblique shocks in this region. Compared with that of Case A, the heat release resulting from the increased fuel injection caused a significant rise of the static pressure, which substantially slows down the local flow around the cavity leading edge. Consequently, the proplonged flow residence time in the cavity shear layer allows fuel and air to be more sufficiently mixed and burnt. Although the quasi-1D analysis suggests the main flow becomes subsonic, we note that the relatively small size of the flame adjacent to the cavity may not be able to cause the thermal choking in the whole flow passage.

In Case C with $\Phi = 0.55$, the flame was observed to reside in the jet-wake from the fuel injector to the cavity downstream, transversely expanded to the whole flow passage in the combustor. Based on the experimentally determined static pressure profile, the quasi-1D analysis suggests that a large amount of heat was produced under such a high equivalence ratio condition and therefore choked the combustor in the upstream of the injector. The thermal choking increases the flow residence time and enhances the fuel/air mixing and combustion, which in turns sustain the choking and thereby the flame.

For Case D with $\Phi = 0.47$, the flame, ocupying a spatial region larger than that of Case B and smaller than that of Case C, was observed to appear partially in the jet-wake and partially in the cavity shear layer. This can be seen from the two distinctly separated regions denoting high standard deviation of flame locations. To further substantiate the observation, the time-resolved CH* images for a duration of 1.8 ms are shown in Fig. 5. It is seen that the flame migrated upstream from within the cavity to the jet-wake and to the injector from 0.0 to 0.8 ms; it subsequently retreated downstream to the cavity from 1.0 to 1.8 ms. The quasi-1D analysis shows that thermal choking occurs around the location of fuel injection. Consequently, a

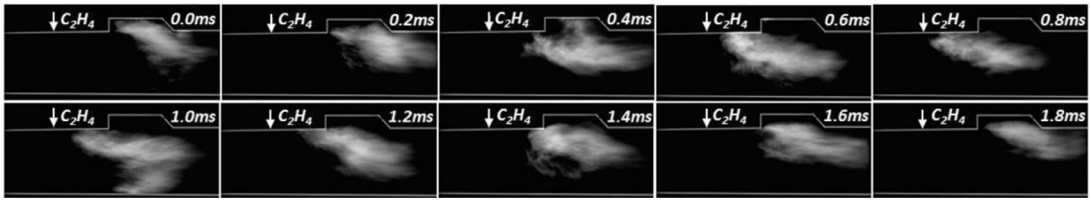


Fig. 5. Time resolved CH* chemilluminesence images in Case D. Exposure time is 100 μs and sampling frequency 5000 fps.

possible explaination for the flame oscillation is that an short-lived aerodynamic throat formed near the injection location due to the fuel combustion may induce the oscillation between the cavity shear layer and jet-wake stabilization modes [12]. Under such conditions of $T_0$ and Φ, the backpressure builtup by the heat release is sufficiently high to choke the combustor but not to stabilize the flame in the jet wake. The flame oscillation synchronizes with the transition between the cavity shear-layer stabilization mode, in which a local subsonic flow exists around the cavity and the main flow remains supersonic, and the jet-wake stabilization mode, in which the entire flow passage is thermally choked due to the large amount of heat release.

To investigate the influence of $T_0$ on the flame stabilization modes, we further considered Cases E and F, which have the same Φ as Case D and an either smaller or larger $T_0$ than that of Case D. In Case E with $T_0 = 1280$ K, the static temperature and therefore the speed of sound of the airflow are reduced from those in Case D. The flame was stabilized in jet-wake as the result of a longer flow residence time, which facilitated the fuel/air mixming and combustion in jet-wake. When the flow speed increased as $T_0$ is increased to 1780 K in Case F, the flame could not be stablized in the jet-wake; it was pushed downstream toward the cavity and stabilized in cavity shear layer. These observations should not be considered to contradict with those reported by Micka and Driscoll [7], where the jet-wake and cavity shear layer flame stablization modes were found only for ramjet mode operations with the hydrogen injection a sufficient distance upstream of the cavity. The different combustor geometry, cavity and fuel injection designs between the present study and Micka and Driscoll's restricts any direct comparison, which however merits future studies.

### 3.2. Regime nomogram of flame stabilization modes

To further quantify the influence of $T_0$ and Φ on the flame stabilization modes, we systematically studied more than forty cases with $T_0$ from 1200 to 1800 K and Φ from 0.1 to 0.8. The identified flame stabilization modes are presented in Fig. 6 as a regime nomogram in the $T_0$–Φ paramter space,

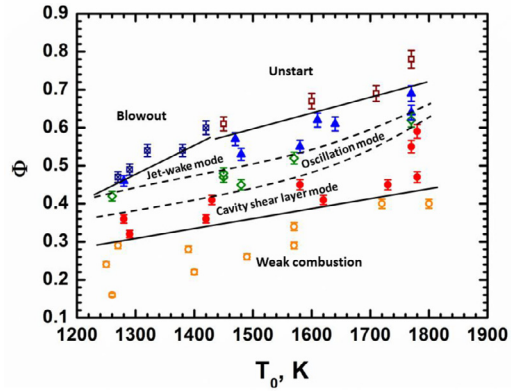


Fig. 6. Regime nomogram of the flame stabilization modes.

in which scattered symbols denote the experimental results and solid lines fitted separation boundaries between different regimes. The corresponding experimental conditions are given in Table S1 of Supporting Material.

By fixing $T_0$ and increasing Φ, the flame was stabilized either in the cavity with weak combustion, or in the cavity shear layer with the main flow remaining supersonic, or in an oscillatory mode transitioning in the cavity shear layer and in the jet-wake, or completely in the jet-wake with the mainflow thermally choked around the location of fuel injection. In the cases with relatively small $T_0$ and large Φ, the flame was blown out because of the relatively low static temperature and excessive fuel, which make the combustion around the fuel injection difficult to sustain. For the cases where both $T_0$ and Φ are relatively large, the substantial amount of heat release cause a significant rise of pressure in the isolator so as to cause the the change of the inlet flow conditions: a case referred to as combustor "unstart". Such "rich" blowout and "unstart" pheomena have been discussed in detail in the recent study of the authors [13].

It is noted that the flame stabilized in jet-wake can only be achieved for the "rich" cases. Given that the Mach number is fixed in the present study, increasing $T_0$ leads to a higher flow velocity and more heat release is needed to choke the flow so as to

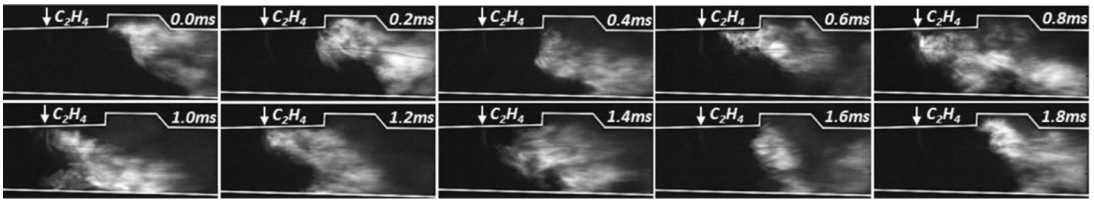


Fig. 7. Time resolved CH* chemilluminesence images in Case D. Exposure time is 39 μs and sampling frequency 25,000 fps.

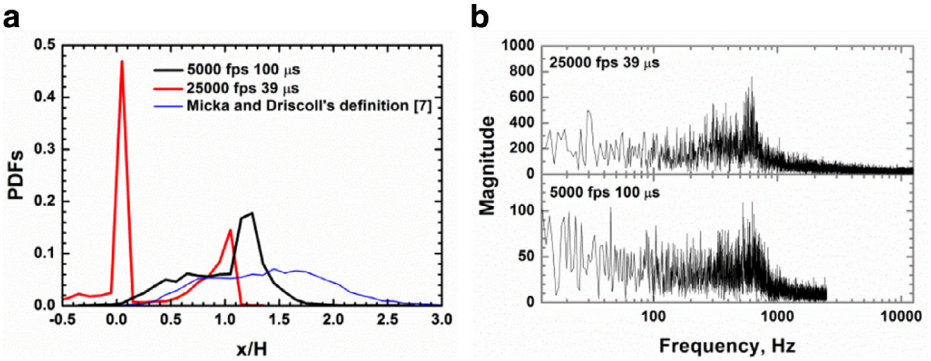


Fig. 8. (a) PDFs of flame locations and (b) FFT of flame locations in Case D.

stablize the flame in the jet-wake. As a result, all the boundaries separating the different flame stablization modes shift to higher Φ as $T_0$ increases. Similar observation was made by Fotia and Driscoll [9] that the jet-wake stabilization mode exists for hydrogen under high stagnation temperature and fueling conditions.

### 3.3. Flame oscillation mode

The characteristics of flame oscillation in Case D was further quantitatively examined through the analyses of probability density function (PDF) and fast Fourier transformation (FFT) on the instananeous flame locations captured by the time-resolved CH* chemiluminescence, as shown in Fig. 7. To compare with and supplement the images in Fig. 5, obtained by using 5000 fps sampling frequency and 100 μs explosure time, Case D was repeated with an augmented frame rate of 25,000 fps and a shorter exposure time of 39 μs. The results consolidate the observations made in the preceding subsecton: the flame migrated from being in the cavity shear layer to being in the jet-wake during 0.0–0.8 ms and the migration process was subsequently reversed during 1.0–1.8 ms.

As shown in Fig. 8a, all the PDFs of flame locations indicate that the flame oscillated in a wide spatial range from the fuel injector (x/H = 0) to the downstream of the cavity leading edge (x/H = 1.0). The PDF of the flame locations, which are determined based on the definition of Micka and Driscoll[7], are also shown in the figure for comparison. Two peaks are clearly seen on the PDF curve for the images with higher temporal resolution: one appears near the cavity leading edge and the other near the position of injection. Such a PDF with two peaks is not seen for the images with relatively lower temporal resolution and for the same images analyzed by using Micka and Driscoll's defintion. The FFT analysis does not suggest a dominant frequency for the flame oscillation, although the preferred frequencies are likely within 500–700 Hz. Due to the same reason indicated in Section 3.1, the preferred frequencies cannot directly be compared with Micka and Driscoll's low frequencies of about 5–20 Hz.

## 4. Concluding remarks

In the present study, flame stabilization modes in an ethylene-fueled supersonic combustor were investigated using time-resolved CH* chemiluminesecence. Defined based on the flame locations, such as inside the cavity, in the cavity shear layer, oscillating between the cavity and jet-wake, and in the jet-wake, four typical flame stabilization modes were identified through the mean and standard deviation images of flame. Particularly, the flame oscillation was visually captured by the time-resolved CH* chemiluminescence with frame rates up to 25,000 fps and exposure times as small as 39 μs.

The flame stabilization modes were systematically mapped as a function of the fuel global euiqvalence ratio and the stagnation temperature. The

boundaries of different modes were found to shift to the higher global equivalence ratio as increasing the stagnaion temperature increases the flow velocity. The correlation between flame stabilization modes and combustion modes were obtained through the average Mach number distributions calculated by using a quasi-1D analysis with the experimentally determined wall static pressure distribution as input paramters. The results show that the flame is stabilized in cavity shear layer when the combustor operates in a scramjet mode; that in jet-wake when the combustor operates in a ramjet mode. These results however need future studies with the help of numerical simulation for characterizing the three-dimensional flow fields around the cavity and fuel injection.

## Acknowledgments

Current research program was supported by the National Nature Science Foundation of China under Contractor No. 91,016,005 and No. 11,502,270. The work at the Hong Kong Polytechnic University was supported by RGC/GRF (PolyU 152,217/14E) and Central Research Grant (G-YBGA). The authors would like to thank Prof. G. Yu and J. G. Li for their helpful discussions, and L. J. Meng and X. S. Wei for their technical support.

## References

[1] J.F. Driscoll, C.C. Rasmussen, *J. Propuls. Power* 21 (6) (2005) 1035–1044.
[2] C.K. Law, Major Research Topics in Combustion, Springer-Verlag, New York, 1992, p. 201.
[3] W.H. Heiser, D.T. Pratt, Hypersonic Airbreathing Propulsion, AIAA Education Series, Washington, D.C., 1994, pp. 197–349.
[4] A. Ben-Yakar, R.K. Hanson, *J. Propuls. Power* 17 (1) (2001) 869–877.
[5] A. Thakur, C. Segal, *AIAA Paper 2006–1380* (2006).
[6] K.Y. Hsu, C.D. Carter, M.R. Gruber, T. Barhorst, S. Smith, *J. Propuls. Power* 26 (6) (2010) 1237–1246.
[7] D.J. Micka, J.F. Driscoll, *Proc. Combust. Inst* 32 (2) (2009) 2397–2404.
[8] H.B. Wang, Z.G. Wang, M.B. Sun, H.Y. Wu, *Int. J. Hydrog. Energy* 38 (2013) 12078–12089.
[9] M.L. Fotia, J.F. Driscoll, *J. Propuls. Power* 29 (1) (2013) 261–273.
[10] M.L. Fotia, *J. Propuls. Power* 31 (1) (2015) 69–78.
[11] D.J. Dalle, J.F. Driscoll, S.M. Torrez, *J. Aircr.* 52 (4) (2015) 1345–1354.
[12] Y.M. Yuan, T.C. Zhang, W. Yao, X.J. Fan, *J. Propuls. Power* 31 (6) (2015) 1524–1531.
[13] T.C. Zhang, J. Wang, L. Qi, X.J. Fan, P. Zhang, *J. Propul. Power* 30 (5) (2014) 1161–1166.
[14] T.C. Zhang, J. Wang, X.J. Fan, P. Zhang, *J. Propuls. Power* 30 (5) (2014) 1152–1160.
[15] J.M. Donbar, J.F. Driscoll, C.D. Carter, *Combust. Flame* 122 (1–2) (2000) 1–19.
[16] JeffreyA. Sutton, JamesF. Driscoll, *Appl. Opt.* 42 (15) (2003) 2819–2828.
[17] D.J. Micka, J.F. Driscoll, *AIAA Paper 2008–5071* (2008).
[18] D.J. Micka, S.M. Torrez, J.F. Driscoll, *AIAA Paper 2009–7362* (2009).
[19] D.J. Micka, J.F. Driscoll, *AIAA Paper 2011–321* (2011).
[20] G. Yu, J.G. Li, J.R. Zhao, D.X. Qian, B. Han, Y. Li, *AIAA Paper 1998–3275* (1998).
[21] Y. Lu, X.Z. Wang, L. Li, et al., *AIAA Paper 2015–3556* (2015).
[22] R. Masumoto, S. Tomioka, K. Kudo, A. Murakami, K. Kato, H. Yamasaki, *J. Propuls. Power* 27 (2) (2011) 346–355.
[23] T. Kouchi, G. Masuya, T.M.S. Tomioka, *J. Propuls. Power* 28 (1) (2012) 106–112.